Mixing in Pipelines with Side and Opposed Tees

ARTICLE *in* INDUSTRIAL & ENGINEERING CHEMISTRY RESEARCH · OCTOBER 2003

Impact Factor: 2.59 · DOI: 10.1021/ie0209935

3 AUTHORS, INCLUDING:

Habib Zughbi
BlueScope Steel
24 PUBLICATIONS **150** CITATIONS

SEE PROFILE

Mixing in Pipelines with Side and Opposed Tees

Habib D. Zughbi,* Zahid H. Khokhar, and Rajendra N. Sharma

Department of Chemical Engineering, King Fahd University of Petroleum & Minerals, Box 124, Dhahran 31261, Saudi Arabia

Numerical and experimental investigations of mixing in pipelines with side and opposed tees are carried out. Cold water flowing in a main pipe is mixed with hot water flowing through a tee. The temperature is measured experimentally to quantify the degree of mixing. The velocity and temperature fields are also solved numerically. The effects of the mesh size, mesh-localized refinement, dependence of the fluid physical properties on temperature, and turbulence model on numerical results were examined. Experimental results show good agreement with corresponding predictions of the numerical model over a relatively wide range of Reynolds number; however, close agreement is harder to obtain in the vicinity of the jet through the tee. The pipe length required to achieve 95% mixing is found to be a function of U_j/U_m. The angle at which the side jet is injected determines whether the jet impinges on the opposite wall and also affects the pipe length required to achieve 95% mixing. This work recommends that industry should not use 90° tees because of possible poor mixing at certain velocity ratios and hard impingement. For pipe diameters ranging from 1 to 16 in., if d_j/d_m is kept constant, then for any velocity ratio the 95% mixing is achieved at a distance corresponding to about the same number of the main-pipe diameters. For opposed jets, numerical convergence was harder to obtain at high Reynolds numbers. Some modifications, including the staggering of the two jets, made it easier for the solution to converge.

Introduction

Mixing problems, such as the design and scale-up of a mixer and quantification of mixing, have been traditionally tackled by using empirical correlations. Although this approach has proven to be satisfactory for many applications, it is rather limited because it neglects the complexity of flow in most mixing applications.

Applications where pipeline mixing with tees is used include low-viscosity mixing such as wastewater treatment and blending of some oils (injection of additives) and petrochemical products. Other applications include blending of fuel gas and mixing of feed streams for catalytic reactors. A tee is formed by two pipe sections joined at a right angle to each other. One stream passes straight through the tee, while the other enters perpendicularly at one side as shown in Figure 1. This flow arrangement is known as the side tee. However, other flow arrangements may be used, such as having the two opposing streams enter coaxially and leave through a pipe that is perpendicular to the entering direction. This is known as an opposed tee and is shown in Figure 2. Multiple tees could also be used as shown in Figure 3. For all designs of pipe tees, mixing takes place in shorter distances compared with distances required for mixing in a pipe with undisturbed turbulent flow. Reviews of pipeline mixing with tees have been presented by Simpson,[1] Gray,[2] and Forney.[3]

More recent studies have been carried out by Liou et al.,[4] who experimentally investigated side-jet injection near a rectangular duct entry with various angles. They obtained a reasonable agreement between laser-doppler velocimetry measurements and numerical computations, with the numerical model underpredicting. Other experimental studies of a jet issuing in an open rectangular channel have been done by Weber et al.[5] and Lam and Xia.[6] Pan and Meng[7] presented an experimental investigation of turbulent flow in a round tee mixer.

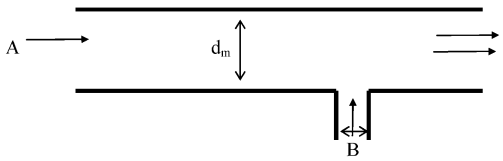

Figure 1. Schematic diagram of a pipeline side tee.

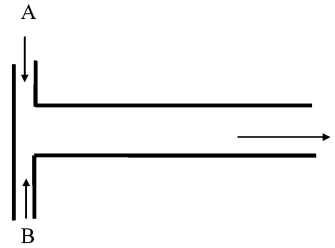

Figure 2. Opposed-tee mixer.

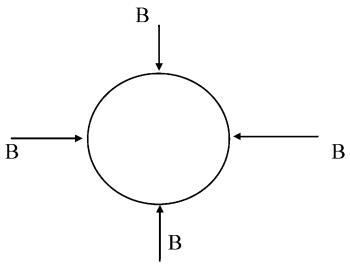

Figure 3. Multiple-tee mixer.

Moussa et al.[8] and Crabb et al.[9] investigated the flows generated by a tee mixer. A survey of the literature shows that simulation using computational fluid dynamics (CFD) of mixing in a pipeline with tees has been carried out by Cozewith et al.[10] and Forney and Mon-

* To whom correspondence should be addressed. E-mail: hdzughbi@kfupm.edu.sa.

10.1021/ie0209935 CCC: $25.00
Published on Web 09/10/2003

clova.[11] Cozewith et al.[10] simulated tee mixing characteristics with and without a reaction for a tee with $d/D = 0.188$ over a range of side-stream/main-stream velocity ratios from 1.2 to 6.5. A three-dimensional model was constructed, and the $k-\epsilon$ model was used to model turbulence. The numerical results of Cozewith et al.[10] were in reasonable agreement with the experimental concentration trajectory found by Cozewith and Busko[12] for $x/D > 0.7$. The concentration trajectory is defined as the locus of maximum concentration. Other comparisons also showed a qualitative agreement between experimental and numerical results.

Forney and Monclova[11] simulated pipeline side-tee mixing quality with the commercially available fluid flow package PHOENICS. The $k-\epsilon$ model was used to model turbulence. Their numerical results satisfactorily matched the experimental results of Sroka and Forney.[13,14]

Both of the above numerical models solved the conservation equations for mass and momentum in primitive variables for steady turbulent flow of a single-phase fluid with an inert tracer introduced at the injection point. The models also used a mixing criteria based on the standard deviation of the component mixed and the mean value of the tracer over the pipe cross-sectional area $\bar{c}$. The use of CFD, despite the above-mentioned investigations, has still a lot to offer in analyzing and understanding mixing in pipeline tees. Simulation of variations of side- and opposed-tee mixers has received limited attention in the literature.

Most of the research done on pipeline mixing has been for a configuration in which the jet is normal to the pipeline. Maruyama et al.[15] carried out experiments for mixing of two fluids at various angles. Feng et al.[16] presented an analytical solution using an asymptotic procedure to evaluate the tracer trajectory in a pipeline with a side tee at various angles. The Feng et al.[16] results were in good agreement with those of Maruyama et al.[15] Feng et al.[16] stated that, in many chemical engineering processes, it is desirable to have the side jet impinge on the opposite wall in order to enhance mixing.

The main interest of this paper concentrates around the side and opposed tees shown in Figures 1 and 2. Mixing of hot and cold fluids is investigated in pipelines with tees. The dependence of the pipe length required to achieve 95% mixing on the side- to main-velocity ratio and the side- to main-diameter ratio is investigated. The effects of the angle of the tee and the use of opposed tees are also investigated.

Model Equations

The differential equations representing mass, momentum, and energy conservation can be written in the general form:

$$\underset{\text{transient}}{\partial(\rho\phi)/\partial t} + \underset{\text{convection}}{\operatorname{div}(\rho\mathbf{U}\phi} - \underset{\text{diffusion}}{\rho\Gamma_\phi \operatorname{grad}\phi)} = \underset{\text{source}}{S_\phi} \quad (1)$$

where ϕ is any conserved property, $\mathbf{U}$ is the velocity vector, Γ_ϕ is the exchange coefficient of ϕ in the phase, S_ϕ is the source rate of ϕ. Thus, the continuity equation, for example, becomes

$$\partial(\rho)/\partial t + \operatorname{div}(\rho\mathbf{U}) = 0 \quad (2)$$

where ρ is the density of the fluid. The conservation of momentum for variable ϕ becomes

$$\operatorname{div}(\rho\mathbf{U}\phi - \mu_{\text{eff}} \operatorname{grad}\phi) = S_\phi \quad (3)$$

where μ_{eff} is the effective viscosity and S_ϕ is the source of ϕ per unit volume. Similarly, the equation of energy can be written.

Experimental Apparatus

The experimental setup used in the current study is shown in Figure 4. Hot water is injected through a $^1/_4$-in. side tee ($^1/_8$ in. has also been used) and is mixed with cold water flowing in a 1-in. main pipe. The temperature is used as the measured variable to quantify mixing. Eight thermocouples are inserted at various positions of the main and side pipes in order to measure the axial temperature of the flow and that of the incoming side flow. The thermocouples are connected via an OMEGA data-logging board to a PC as shown. Flow through the side tee passes through a heater that can raise the temperature of the side stream significantly above that

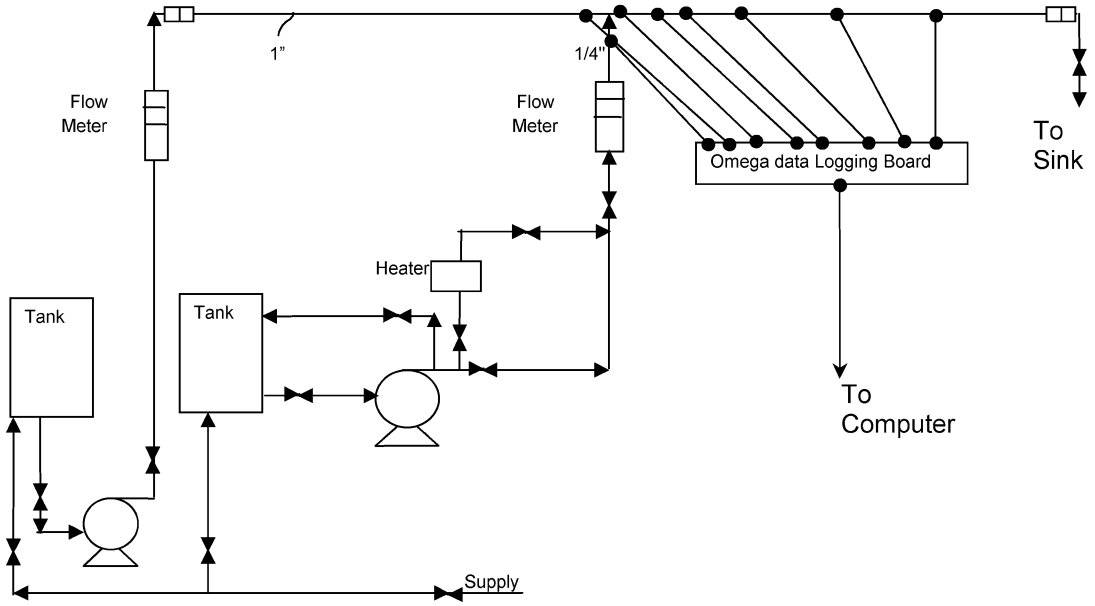

Figure 4. Schematic diagram of the experimental rig used to investigate mixing of a pipeline with a side tee.

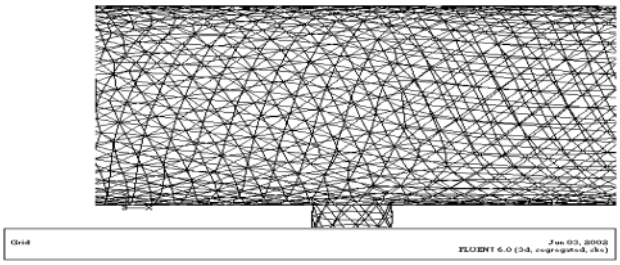

Figure 5. Computational grid of a piece of the main pipe with a side tee used in the present simulations.

of the main stream. The flowmeters on each of the flow streams allow varying flow rates in the main and side pipes. Details of the flow rates, temperatures, and diameters used are given in a later section.

Numerical Model

Flow in a pipeline is simulated by solving the mass and momentum conservation equations. The degree of mixing is investigated by solving the energy equation and by monitoring the temperature at various positions along the flow. The general purpose three-dimensional CFD package FLUENT is used to solve the governing equations. This allows the investigation of a range of conditions and geometries quite efficiently once a general model has been established and validated against experimental results.

A three-dimensional numerical model representing a main pipe with a side tee was constructed. A part of the grid is shown in Figure 5. An unstructured tetrahedral grid was chosen. A base case was used to test the dependence of the numerical solution on the grid size and to test the effects of various turbulence models.

In this study, the pipe length required to achieve 95% mixing is numerically and experimentally determined. This is the length from the jet inlet to the location along the pipe where the value of the measured quantity anywhere in the pipe is less than 5% of the step input. The step input is defined as the difference between the initial value and the final mean value.

In terms of a concentration tracer, m can be defined as

$$m = \left|\frac{c - \bar{c}}{\bar{c}}\right| < 0.5$$

where $\bar{c}$ is the equilibrium concentration and c is the concentration at any monitoring point at any time. When the above condition is met at all monitoring points in a cross-sectional plane of the main pipe, it can then be said that the concentration at any point of the pipe after that length has reached 95% or more of the equilibrium concentration.

Other researchers defined uniformity criteria in terms of the second and third moments about the arithmetic mean of an inert tracer at a given tube cross-sectional area. The second moment about a mean value is defined for a given tube cross section A in the form

$$m_2 = \int_A (c - \bar{c})^2 u \, dA / \int_A u \, dA$$

In the present study, the flow in the main pipe before the jet inlet is set initially at a certain temperature. The flow through the side tee is set at a higher but known temperature. Because the flow rate and temperature of the main and side streams are known, the equilibrium temperature of the combined stream, $\bar{T}$, can be calculated. The 95% mixing is reached when the temperature anywhere across a plane inside the pipe is within the range of $\bar{T} \pm (\bar{T} - T_{im}) \times 0.05$, where T_{im} is the initial temperature of the fluid in the main pipe, i.e., before the inlet of the side tee. The length required for the hot fluid to mix is then measured according to this criterion, which means that the maximum temperature difference between any two points across a cross-sectional area of the pipe should not exceed a certain value, which is a function of the initial temperatures and the flow rates of the fluids in the main and side pipes.

Results

The numerical and experimental results of mixing in pipelines with side and opposed tees are presented in this paper. Numerical results are first tested for dependence on the mesh size, turbulence model, and location of the tee, and then a detailed comparison of the numerical and experimental results is presented.

A base case consisting of a 15-in.-long piece of a 1-in. main pipe, with a side pipe of $^1/_4$ in. connected at 2 in. from the entry end of the main pipe, is chosen. At the entry end of the main pipe, a flow rate of liquid water, Q_m, of 9 L/min is used, and through the side pipe, a flow rate of water, Q_j, of 7 L/min is used. These flow rates result in a velocity ratio (U_j/U_m) of 17.1. The temperature of the water in the main pipe is around 10 °C, while the temperature of the water in the side pipe is around 50 °C. A mesh size of 2 mm is used, and turbulence is modeled by using the standard $k-\epsilon$ model.

Figures 6 and 7 show the velocity and temperature contours in a plane along the pipe axis for this case. Figure 6 shows clearly that the jet impinges on the opposite wall of the pipe. From the temperature contours displayed in Figure 7, it can be seen that the distance for 95% mixing to be achieved is about 9 in. or 9 pipe diameters. To analyze the results quantitatively, the values of temperature versus location along the pipe axis are plotted. To validate the numerical model, these numerical values will be compared in a later section with experimental values measured at exactly the same locations.

At very low velocity ratios, the jet does not impinge on the opposite wall and the high-pressure point is at the inlet of the tee. For higher velocity ratios, the side jet impinges on the opposite wall of the pipe and creates a region of backflow. The high-pressure point is transferred to the opposite wall downstream of the axis of the jet, while upstream of the jet, there is a zone of very low velocity.

Before numerical results are compared with experimental results, the dependence of the numerical solution on the grid size, turbulence model, and other factors is first tested.

Dependence of Solution on the Grid Size

The mesh size often has an impact on the accuracy of the solution. The size has to be small enough in order to properly resolve the fields that are solved for. To quantitatively compare the results with different sizes, mesh sizes of 4, 3, and 2 mm have been tested. The number of cells used for mesh sizes of 4, 3, and 2 mm are 18 610, 56 463, and 162 367 cells, respectively.

The effects of the mesh size are tested by comparing a plot of the temperature versus location along the

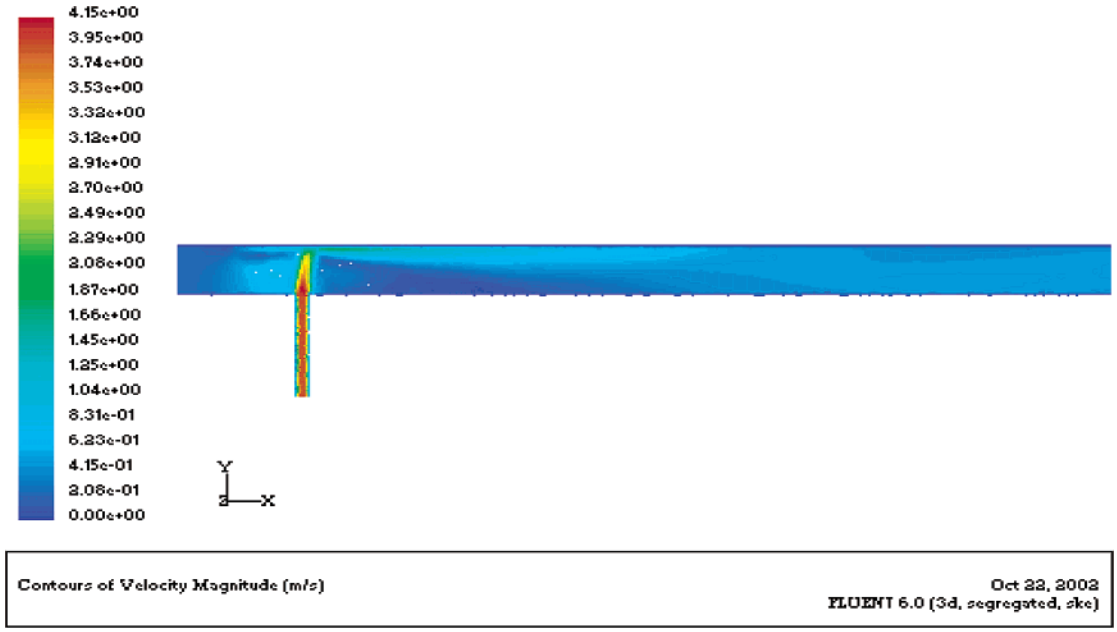

Figure 6. Velocity contours in a plane passing through the centerline for a mesh size of 2 mm.

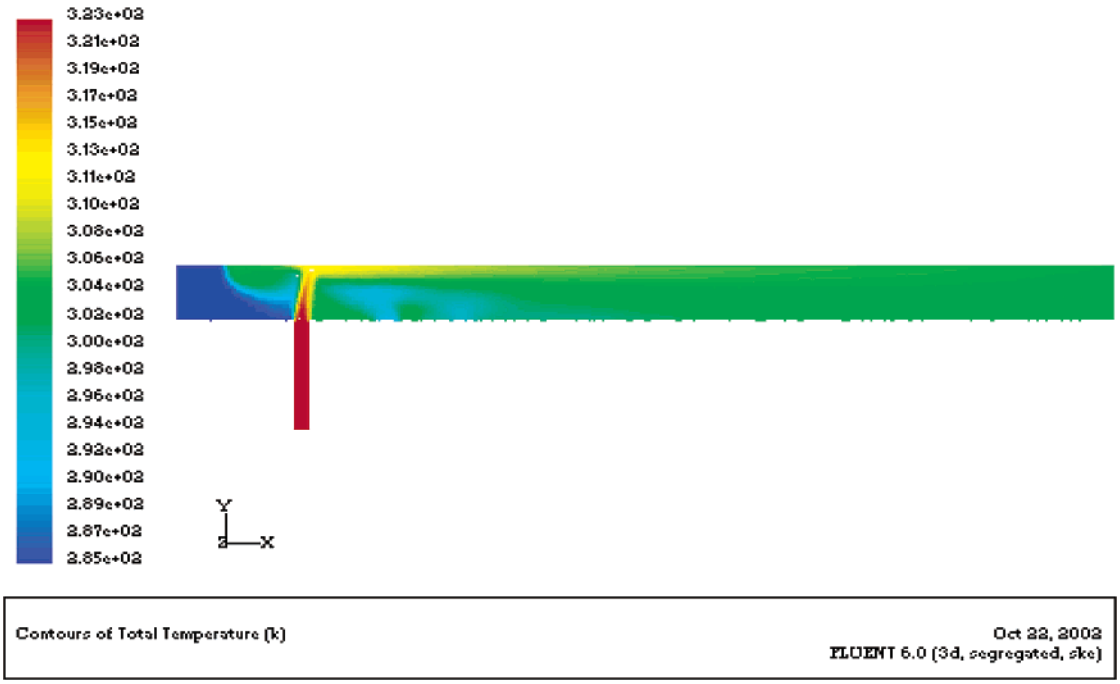

Figure 7. Temperature contours in a plane passing through the centerline for a mesh size of 2 mm.

center line of the main pipe. Figure 8 shows such a comparison for the three mesh sizes considered with turbulence modeled using the $k-\epsilon$ model. It is clear that the solution shows a significant change when the mesh size is reduced from 4 to 3 mm. The solution also changes when the mesh size is further reduced from 3 to 2 mm, but the difference between solutions of mesh sizes of 3 and 2 mm is not very significant. The number of cells for a mesh size of 2 mm is relatively very high; however, because the solution still shows some change, a mesh size of 1 mm was attempted. This attempt could not be completed because the time required to perform the meshing of the computational domain is prohibitively excessive. Therefore, a mesh size of 2 mm was used for all of the main runs in this study.

Figure 9 shows a comparison of the numerical results using the Reynolds stress model (RSM) of turbulence for mesh sizes of 2 and 3 mm. A small difference is observed mainly around the jet zone.

Grid Refinement

The grid is locally refined especially in the area where the gradient of temperature and velocity is high. A temperature gradient of 0.001 K/m was used as the basis for mesh refinement. This refinement increased the number of cells from 162 367 to 183 161. A further refinement was introduced, and the number of cells became 215 893 cells when a gradient of 0.0005 K/m was used.

An adapted grid is shown in Figure 10. More cells can be seen along the boundary of the jet, where the

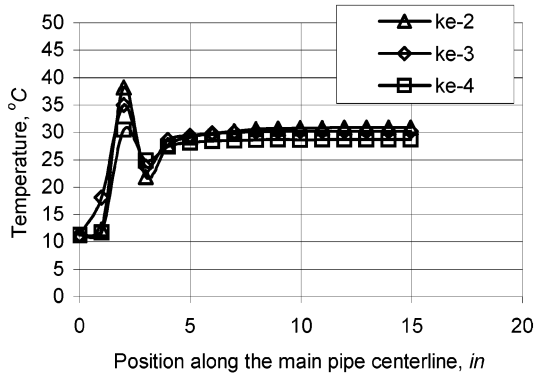

Figure 8. Comparison of the temperature profile along the center of the main pipe for mesh sizes of 4, 3, and 2 mm.

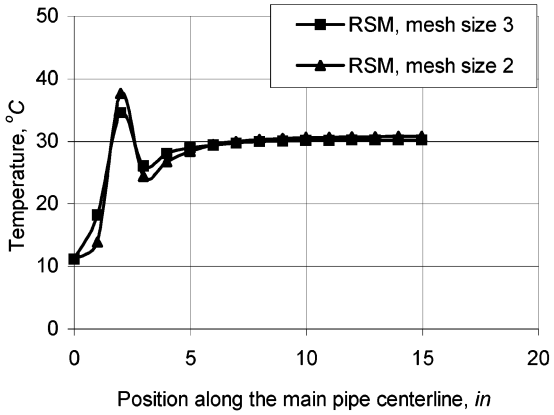

Figure 9. Comparison of temperature versus location along a centerline for mesh sizes of 2 and 3 mm using the RSM.

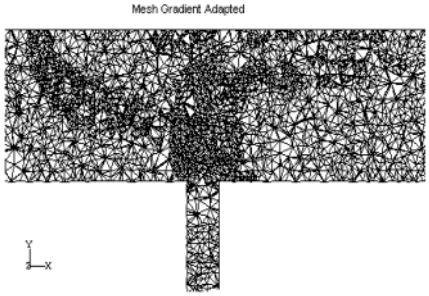

Figure 10. Computational grid following refinement where the velocity gradient is high. These zones have smaller mesh cells.

temperature gradient is greatest. Temperature profiles along a centerline of the main pipe are shown for all three cases in Figure 11. This figure shows that the temperature profile along the center of the pipe away from the jet is almost identical for all three cases; however, for the jet zone the temperature profile shows certain differences, and the use of the finest adaption is recommended if the interest is concentrated in the jet zone. Increasing the number of cells by 41% results in a large increase in the CPU time required for convergence.

Fully Developed versus Developing Flows

The lengths of the main and side pipes upstream of the tee location required to ensure that the flow in the main and side pipes is fully developed are numerically tested in this subsection. First a main-pipe section of 15 in. is used with the tee located 2 in. downstream from the water inlet. The tee length is taken to be 2 in. long

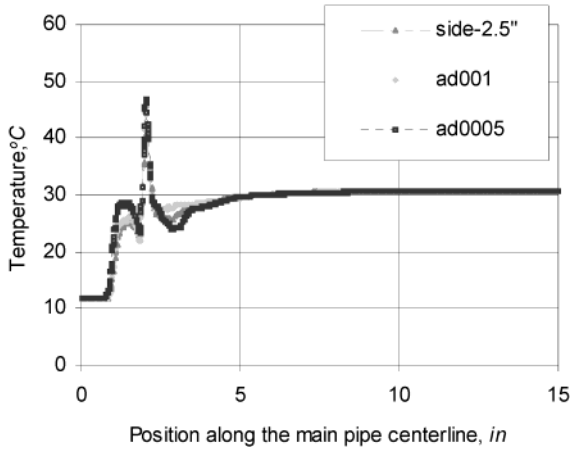

Figure 11. Comparison of temperature profiles for cases with no grid adaption and with grid adaption using gradients of 0.001 and 0.0005 K/m.

also. The total length of the main-pipe section has been changed to 18 in. and then 21 in., which corresponds to a tee location of 5 and 8 in. away from the entry point. Results are shown in Figure 12. Results show that the temperature profile along a centerline of the main pipe away from the jet is almost identical. Near the jet, minor differences in the temperature profile are observed.

Similar tests were done on the side-pipe section of 2 and 4 in. (corresponding to 8 and 16 diameters). Results are shown in Figure 13, and no significant difference was observed between the two cases.

It can be concluded that a numerical model to predict the length of the pipe needed to achieve 95% mixing needs many refinements if a good agreement is required between the numerical and experimental results near the jet zone.

Turbulence Modeling

Many researchers have recommended and used the $k-\epsilon$ model to simulate turbulence in mixing studies. Cozewith et al.[10] and Forney and Monclova[11] used this model for their mixing in pipeline studies; Jayanti,[17] Zughbi and Rakib,[18] and Patwardhan[19] also used the $k-\epsilon$ model in investigations of mixing in fluid-jet-agitated vessels. In general, the $k-\epsilon$ model proved to be satisfactory. In this study, simulations are carried out using the $k-\epsilon$ model and the RSM.

Figure 14 shows a comparison of the numerical results for a base case with these two models of turbulence. It shows that both the RSM and the $k-\epsilon$ model predicted the same value of the pipe length required to achieve 95% mixing. However, for the results in the vicinity of the incoming jet, a significant difference in the results is observed. The RSM gives a better estimate of the temperature profile in the vicinity of the jet.

The computational time required when using the RSM is about 3 times that when using the $k-\epsilon$ model. However, because this study attempts to analyze the results near the jet as well as calculate the pipe length required for 95% mixing, the RSM and the $k-\epsilon$ model are used. Another option would have been to change the constants in the $k-\epsilon$ model to get a better fit. However, Patwardhan[19] reported a limited improvement by this technique.

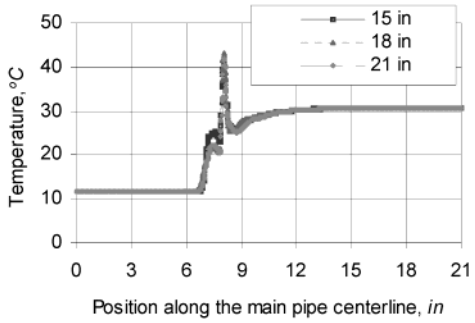

Figure 12. Temperature profiles along the central axis of the main pipe for various main-pipe lengths.

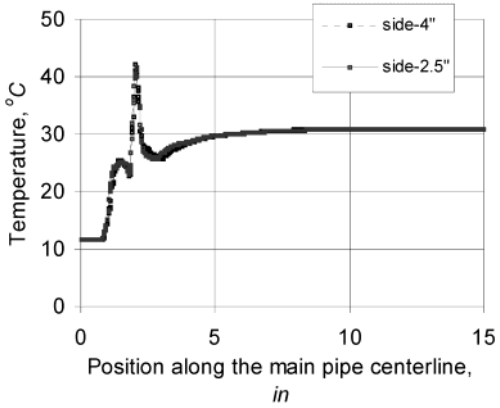

Figure 13. Temperature profiles along the main-pipe axis for two different lengths of the side pipe.

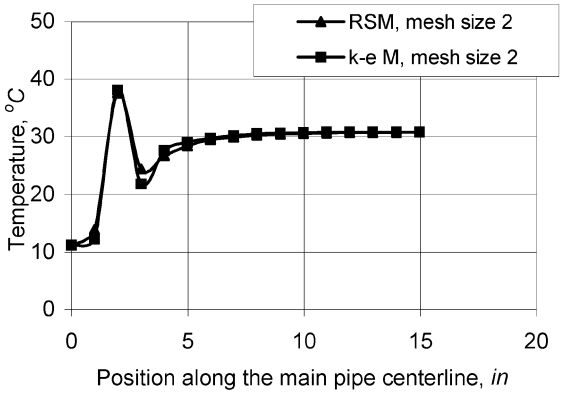

Figure 14. Plots of temperature versus location along the centerline of the main pipe for cases with the $k-\epsilon$ model and the RSM.

Effect of the Dependence of Physical Properties of Liquid Water on Temperature

The numerical results are obtained using constant values of the density, viscosity, and heat capacity of water. These three properties are a function of temperature. Another numerical run was carried out with the dependence of these physical properties on temperature taken into consideration. The results are shown in Figure 15. The results show that the temperature profile along a centerline of the main pipe does not show any significant difference. The only difference observed is a little increase in the final equilibrium temperature. This is expected because values of the heat capacity increase with an increase in the temperature. The effects of variations in the values of the density and viscosity due to a change in the temperature do not seem to be significant. The dependence of the viscosity, density, and heat capacity on the temperature should only be taken into consideration when a very fine comparison of the results near the jet is required.

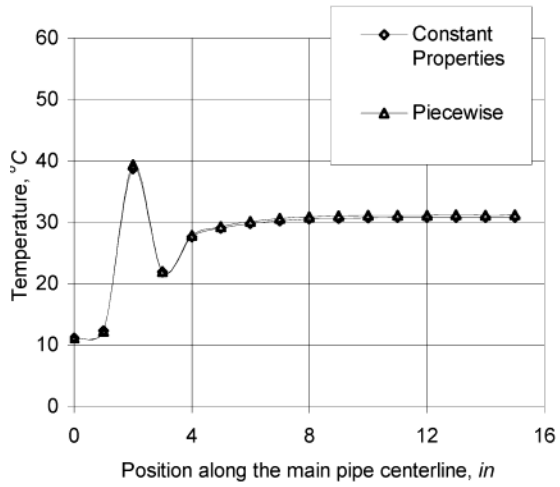

Figure 15. Comparison of numerical results for cases with the density, viscosity, and heat capacity as independent parameters and as a function of temperature.

Effect of the Angle of the Tee

On the basis of the experimental and numerical results, it was observed that, at certain values of the diameter and velocity ratios, the jet impinges on the opposite wall of the main pipe and a region of backflow is thus created. Some researchers stated that impingement might be desirable in some cases in order to enhance rapid mixing (Feng et al.[16]). However, in the paper industry, the tracer is often injected at an angle θ ($45° \leq \theta \leq 60°$) to avoid impingement and to minimize pressure pulsation. The suggestion that a jet impingement results in rapid mixing is a suggestion that may not always be correct according to the studies presented in this paper.

Numerical simulations of mixing in a pipeline with a side tee at a number of angles ranging from 5 to 175° were carried out. All parameters were kept the same except for the angle of the side tee. Results show that the jet impinges at the opposing wall only for a number of angles including 90 and 60°. Figure 16 shows the temperature field for a selected number of angles. These results show that changing the angle of the side tee has very significant results on mixing. Figure 17 shows the temperature profile along the center of the main pipe for a selected number of angles, namely, 30, 45, 60, and 90°. This shows that mixing is achieved faster (over a shorter distance) when an angle of 45 or 60° was used. Using a 30 or 90° angle resulted in slower mixing. This shows that there is an optimum tee angle for which the mixing is fastest.

Figure 18 shows a plot of the length of the pipe needed to achieve 95% mixing as a function of the angle of the tee. These results show that the angle of the tee will determine whether the jet impinges on the opposite wall and will also affect the length needed to achieve mixing. 95% mixing was achieved at a distance of 3 main-pipe diameters for an angle of 45° and at a distance of 3.5 diameters for an angle of 165°. For all other angles, longer pipe lengths were required. A distance of 11 diameters was needed when an angle of 90° was used. Therefore, using the correct angle of injection for a

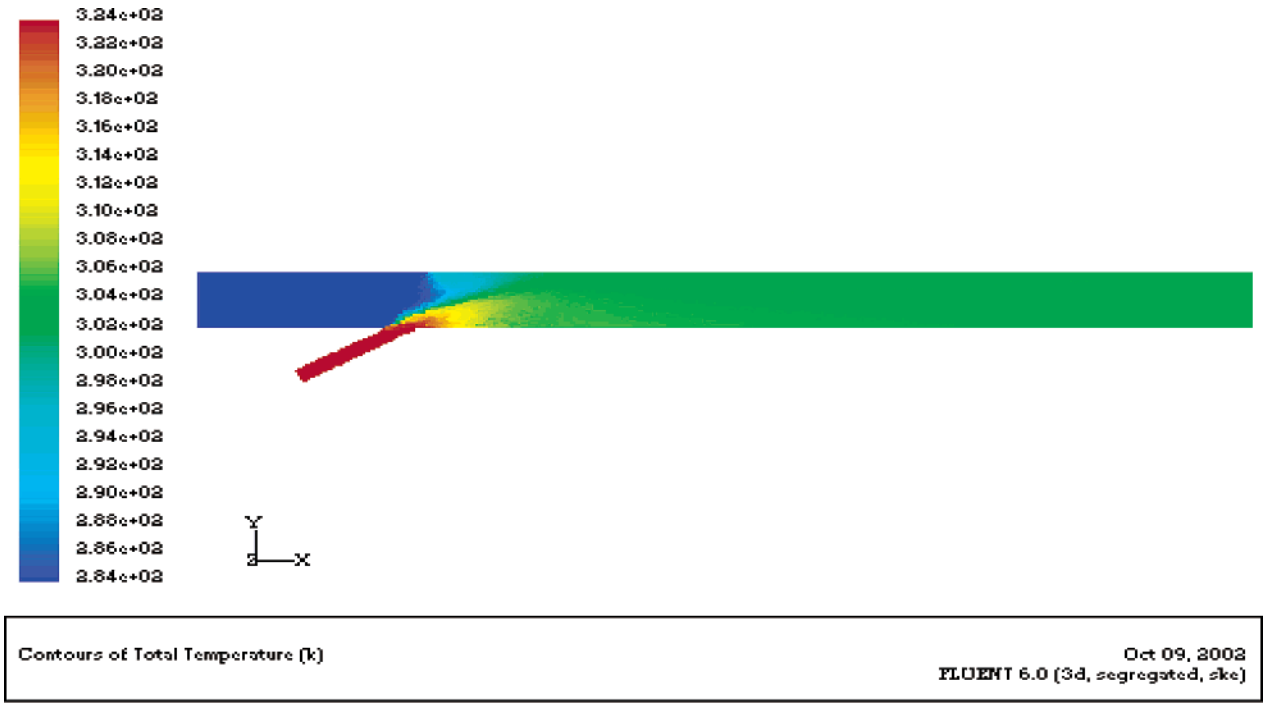
3.24e+02
3.22e+02
3.20e+02
3.18e+02
3.16e+02
3.14e+02
3.12e+02
3.10e+02
3.08e+02
3.06e+02
3.04e+02
3.02e+02
3.00e+02
2.98e+02
2.96e+02
2.94e+02
2.92e+02
2.90e+02
2.88e+02
2.86e+02
2.84e+02
Y
X
Contours of Total Temperature (k)
Oct 09, 2002
FLUENT 6.0 (3d, segregated, ske)

(a)

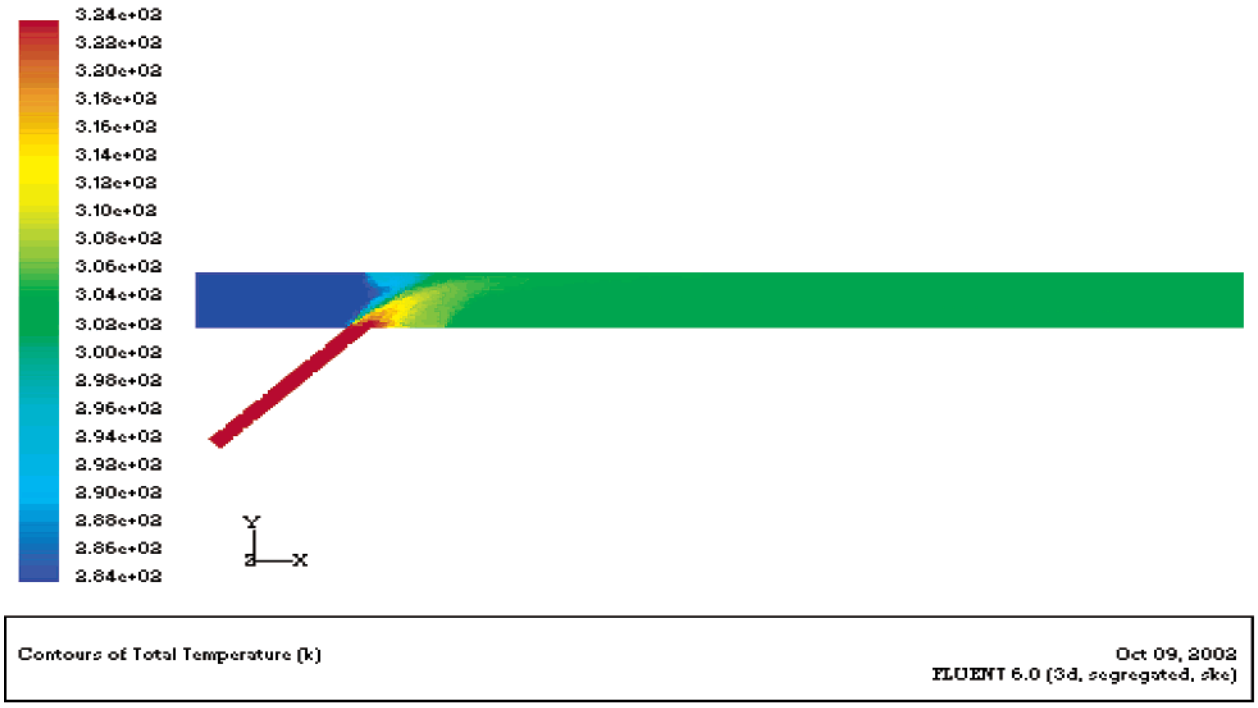
3.24e+02
3.22e+02
3.20e+02
3.18e+02
3.16e+02
3.14e+02
3.12e+02
3.10e+02
3.08e+02
3.06e+02
3.04e+02
3.02e+02
3.00e+02
2.98e+02
2.96e+02
2.94e+02
2.92e+02
2.90e+02
2.88e+02
2.86e+02
2.84e+02
Y
X
Contours of Total Temperature (k)
Oct 09, 2002
FLUENT 6.0 (3d, segregated, ske)

(b)

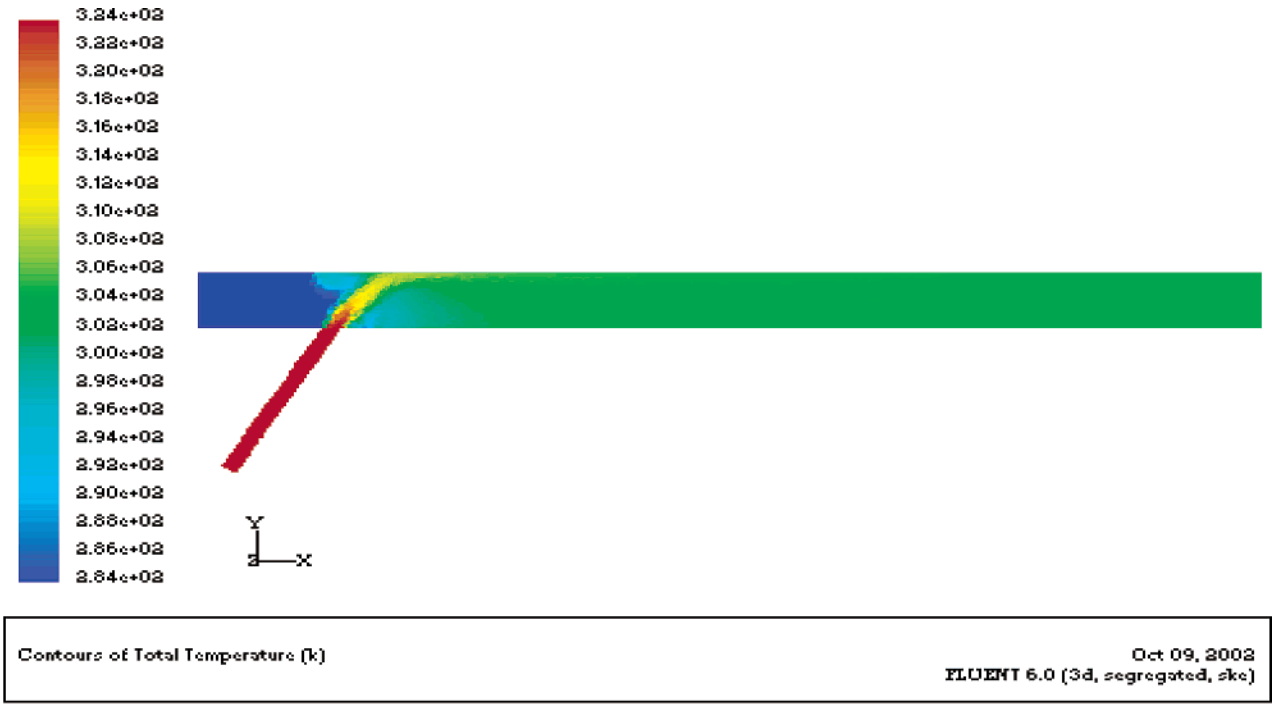

(c)

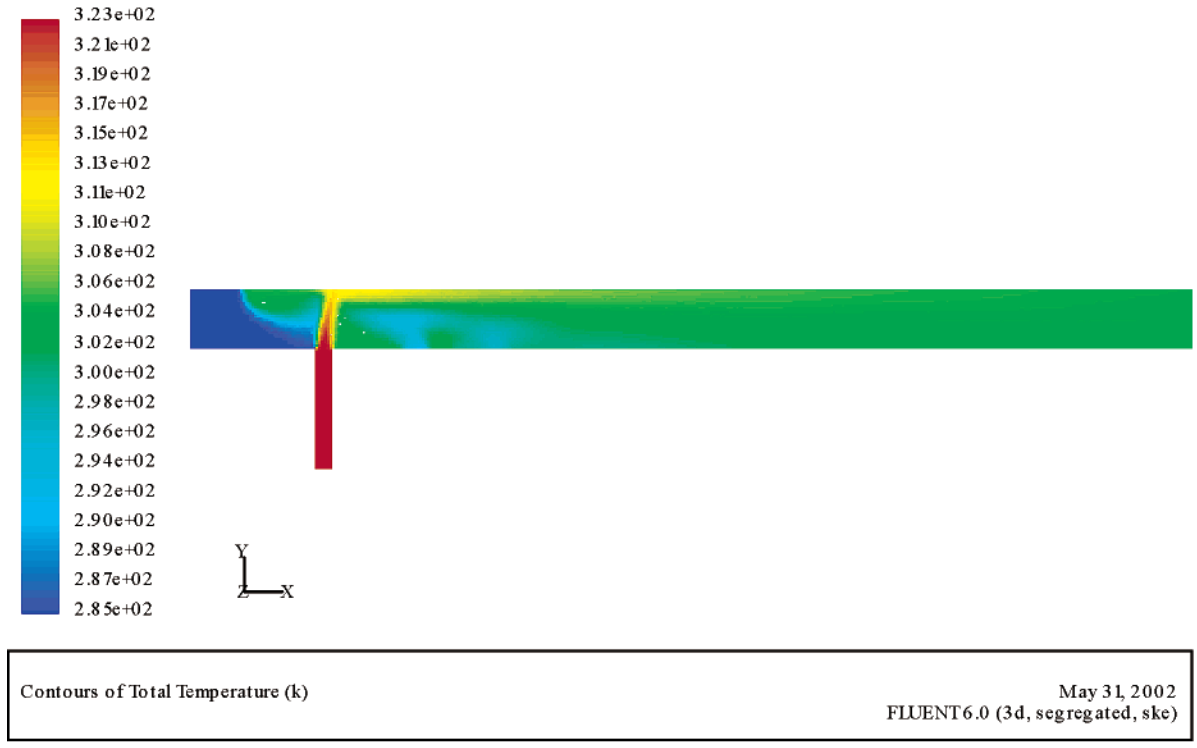

(d)

Figure 16. Temperature flow fields for tee angles of 30, 45, 60, and 90°, respectively.

velocity ratio of 17.1, the 95% mixing length was reduced from 11 to 3 diameters.

On the basis of the above results, it is clear that there is very little incentive for the industry to use 90° tees because these are likely to give the worst results in terms of mixing and possible corrosion and erosion problems.

Experimental Results and Validation of the Numerical Model

Experimental runs have been carried out with water flow rates through the main pipe of 7.02, 12.28, and 19.30 L/min and water flow rates through the side pipe of 7.5, 5.0, and 3.0 L/min. The side-tee diameter is $^1/_4$ in. Details of these runs, together with the correspond-

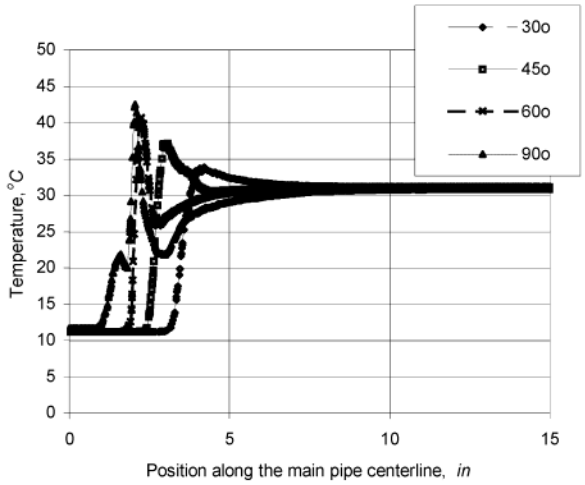

Figure 17. Temperature profile along the axis of the main pipe for tee angles of 30, 45, 60, and 90°.

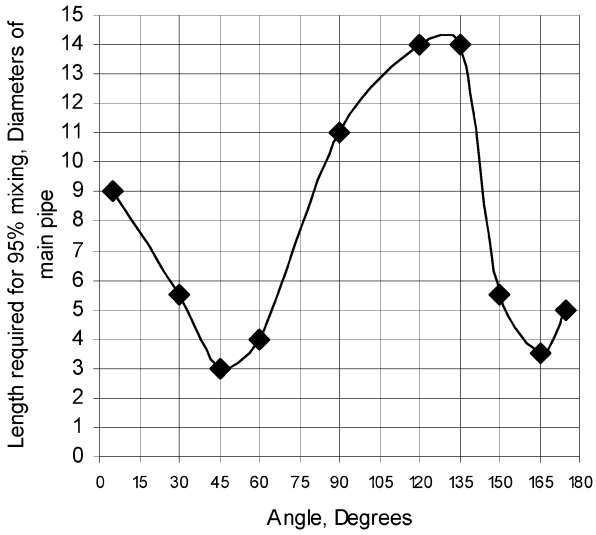

Figure 18. Plot of the distance required to achieve 95% mixing versus the angle of the side tee.

Table 1. Mixing Length for Different Velocity Ratios for a $^1/_4$-in. Side Tee

case	U_j (m/s)	U_m (m/s)	U_j/U_m	T_j (K)	T_m (K)	T_e (K)	mixing length (diameter of the main pipe)
1	3.94	0.63	6.2	283.0	323.0	295.4	11.5
2	3.94	0.40	9.8	283.0	323.0	298.8	12
3	3.94	0.23	17.1	283.0	323.0	303.5	11
4	2.60	0.63	4.1	283.0	323.0	291.8	13-NC[a]
5	2.60	0.40	6.5	283.0	323.0	293.2	13
6	2.60	0.23	11.4	283.0	323.0	299.0	9
7	1.58	0.63	2.5	283.0	323.0	286.0	13-NC[a]
8	1.58	0.40	3.9	283.0	323.0	289.8	13-NC[a]
9	1.58	0.23	6.8	283.0	323.0	294.8	11
10	5.75	0.23	25	283.0	323.0	305.7	6
11	3.45	0.23	15	283.0	323.0	301.6	11.5

[a] Not complete; 95% mixing until 13 diameters.

ing values of the velocity in the side stream U_j, velocity in the main pipe, U_m, ratio of U_j/U_m, and values of the Reynolds number in the side and main pipes before and after the tee, are given in Table 1.

These results are plotted in Figure 19. The data show a certain amount of scatter especially for velocity ratios of less than 20. Similar data for the same main pipe and a side-tee diameter of $^1/_8$ in. are plotted in Figure 20. A much clearer trend and significantly less data scatter are observed.

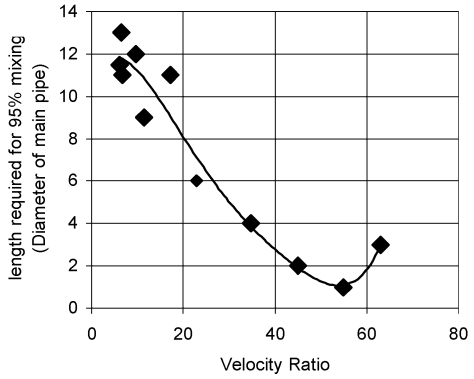

Figure 19. 95% mixing length in diameters of the main pipe versus U_j/U_m, for 95% completely mixed cases for a $^1/_4$-in. right-angled side tee.

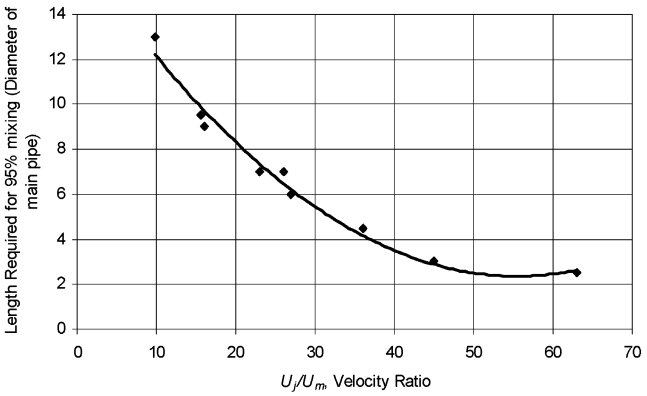

Figure 20. 95% mixing length versus U_j/U_m for all cases for an $^1/_8$-in. right-angled side tee.

Figure 19 shows how the 95% mixing length changes with an increase in the velocity ratio. At low velocity ratio, the jet impinges on the opposite wall and connects with that wall. This means that the jet is not centered and 95% mixing requires a long distance. As the velocity increases, the jet starts to bounce back off the opposite wall, and at a ratio of about 55, the jet becomes centered after its impingement. The 95% mixing length starts to increase as the velocity ratio is further increased. This is because the jet starts to move further away from the center. This phenomenon is shown schematically in Figure 21.

Figure 22 shows plots of the temperature measured by the thermocouples versus the location along the centerline of the main pipeline for the three cases. From the figure, the discrepancy between the numerical and experimental results near the jet is due to the fact that the grid adaption used in this case does not correspond with the low values of the gradients. However, good agreement is observed away from the jet. When all of the numerical enhancements were included in the model, excellent agreement was obtained, as shown in Figure 23. Similar agreement between the experimental and numerical results was obtained for all other cases.

Mixing in a Pipeline with Opposed Tees

Numerical simulations of a pipeline with opposed tees have been carried out. Some difficulties were experienced when two directly opposite jets were injected. This is due mainly to jet−jet interaction. However, with some modifications, geometries shown in Figure 24, converged

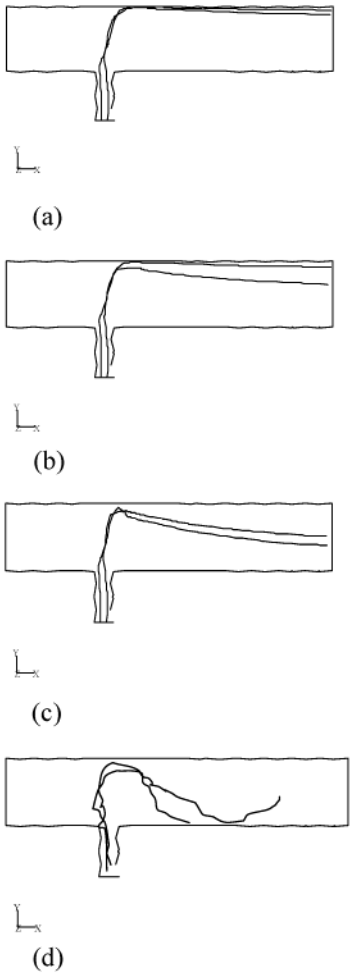

Figure 21. Pathline diagram of a side jet bending into the main fluid as U_j/U_m is increased: (a) low U_j/U_m; (b) low to medium U_j/U_m; (c) high U_j/U_m; (d) very high U_j/U_m.

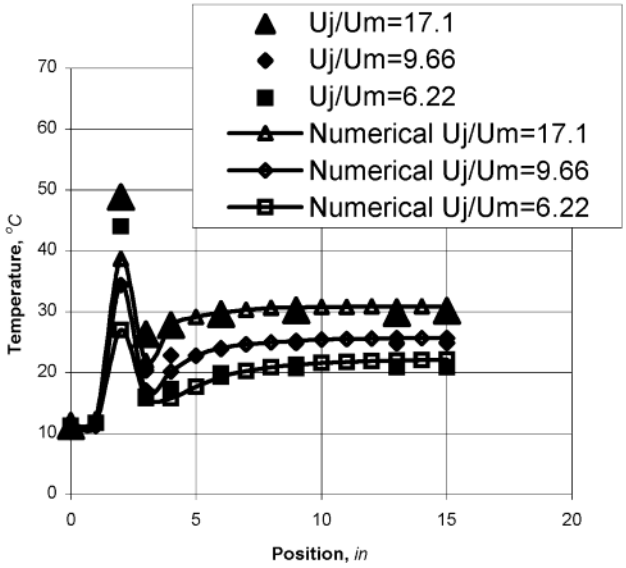

Figure 22. Plot of experimental and simulated, using the $k-\epsilon$ model, values of temperature versus location along the centerline of the main pipe for cases with Q_m of 7.02, 12.28, and 19.3 L/min and Q_j of 7.5 L/min.

results were obtained. One case for which results were obtained is shown in Figure 25, where the two tees are opposed but one side-pipe diameter is much larger than the other one. This figure shows that mixing takes place,

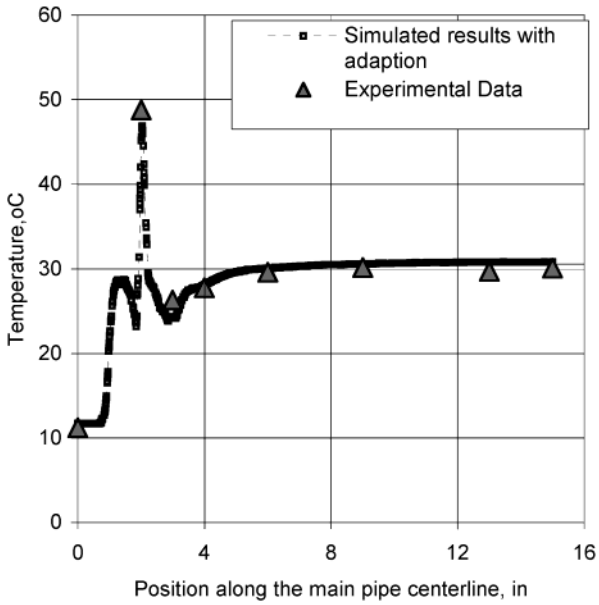

Figure 23. Comparison of experimental results with numerical results with a grid adaption (refinement) using a gradient of 0.0005 K/m for a velocity ratio of U_j/U_m of 17.1.

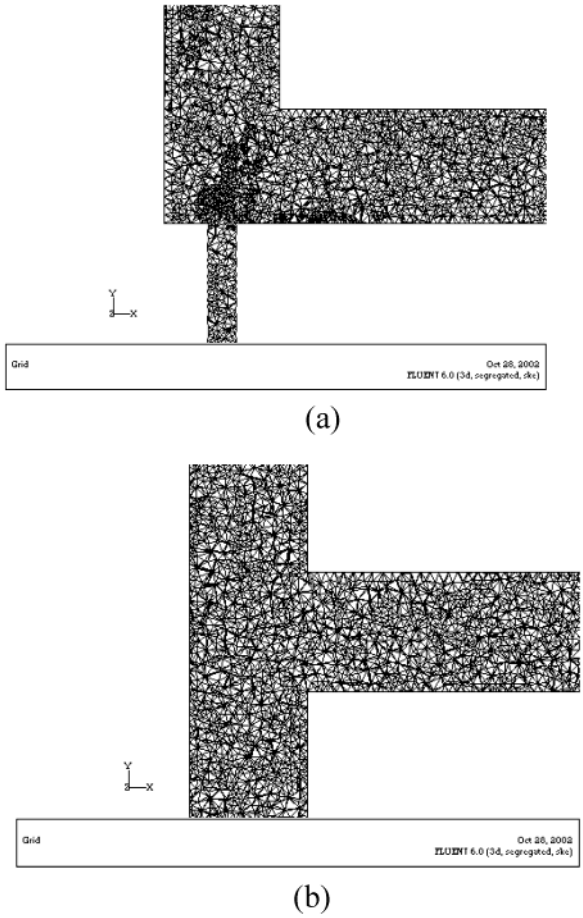

Figure 24. Arrangements for opposed tees for which a converged solution was obtained.

in fact, faster (5.5 diameters) than when using one 90° side tee (11 diameters) for U_j/U_m of 17.1. A slight movement of the jet position in the positive or negative x direction caused the solution to diverge. It should be mentioned that an inclined tee gave even better results than opposed tees.

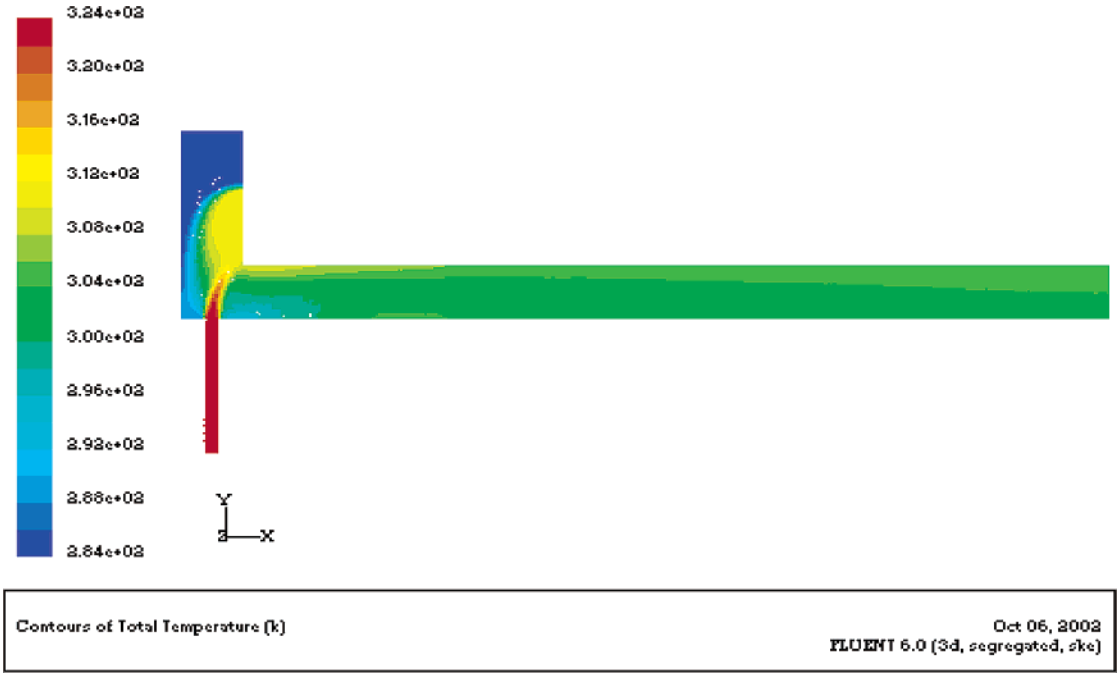

Figure 25. Temperature contours for an opposed-tee arrangement.

Table 2. Comparison of 1 in.−1/4 in. and 4 in.−1 in. Cases Keeping the Reynolds Number Constant

flow rate kept constant	*Re*, Reynolds number	old *Q* flow rates (L/min)	velocity (m/s)	diameter (in.)	scale-up diameter (in.)	new flow rate (L/min)	new velocity (m/s)
main	5842.0	7.01	0.23	1	4	28	0.06
jet	66802.0	19.99	10.52	0.25	1	80	2.63
ratio, jet/main	5.7	2.9	45.7	0.25	0.25	2.9	45.7

Table 3. Comparison of the Pipe Length Required for 95% for 1 in.−$^1/_4$ in. and 4 in.−1 in. Cases Keeping the Velocity, Flow Rate, and Reynolds Number Constant with Base Case

			length required, from entrance of side jet, for 95% mixing	
case D_m-d_j	Re_{mixed}	U_j/U_m	in.	diameters of the main pipe
1 in.−$^1/_4$ in. base case	22 542.5	45.7	3	3
4 in.−1 in., velocity constant	90 170	45.7	9	2.25
4 in.−1 in., flow rate constant	5 639.3	45.7	9	2.25
4 in.−1 in., Reynolds number constant	22 542.5	45.7	9	2.25

Mixing in Larger Diameter Pipes: Scale-up

In the previous sections, mixing in a 1-in. main pipe with side tees of $^1/_4$ and $^1/_8$ in. was investigated. Mixing in larger pipe diameters with tees was also investigated. Geometric scale-up factors of 4 and 16 were used. This means that, in addition to the base case of 1 in.−$^1/_4$ in. arrangement, two similar arrangements of dimensions 4 in.−1 in. and 16 in.−4 in. were numerically investigated.

Numerical models of these geometries were constructed. A number of simulations were carried out until the solution was independent of the grid size.

For the 4 in.−1 in. case, mesh sizes of 10, 8, and 7 mm were used, corresponding to 80 334, 171 770, and 222 794 cells, respectively. The solution was found to be grid-independent with a mesh size of 7 mm. For the 16 in.−4 in. case, mesh sizes of 50, 25, and 20 mm were used, corresponding to 40 920, 356 549, and 618 222 cells, respectively. The solution was found to be grid-independent with a mesh size of 20 mm.

The pipe length required to achieve 95% mixing was calculated for each of the above three cases for a range of jet- to main-velocity ratios (U_j/U_m). The velocity in the main pipe U_m is kept constant at 0.23 m/s, while U_j is varied between 3.933 and 14.95 m/s. A plot of the 95% mixing length versus the velocity ratio U_j/U_m is shown in Figure 26. Results show that, for the same velocity in the main pipe, the 95% mixing length decreases as

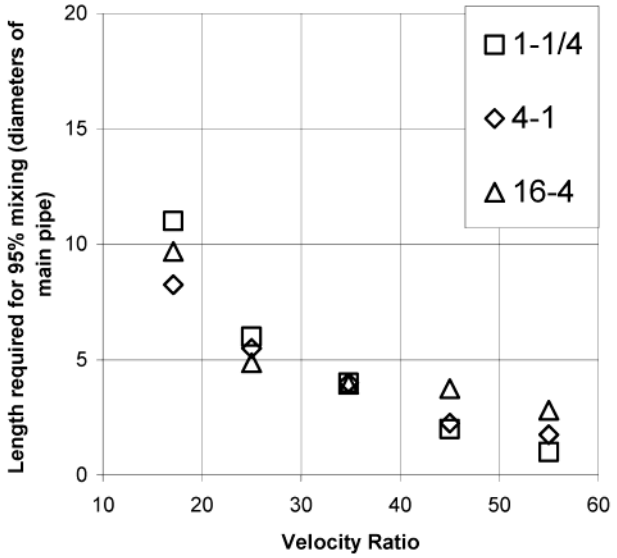

Figure 26. Plot of 95% mixing length for various pipe sizes versus jet- to main-velocity ratios.

the velocity ratio increases. However, for the same side- to main-diameter ratios, the mixing length does not vary significantly. This means the length of the pipe required for 95% mixing to be achieved in 1 in.−$^1/_4$ in., 4 in.−1 in., and 16 in.−4 in. is about the same in diameters of the main pipe. For velocity ratios smaller than 35, 95% mixing increased marginally as the sizes of the pipe decreased. This trend was reversed for velocity ratios larger than 35.

On the basis of these results, it can be concluded that the mixing length is a strong function of the velocity ratio (U_j/U_m) and the jet- to main-pipe-diameter ratio (d_j/d_m). The actual size of the pipes does not have a major impact on the 95% mixing length.

To investigate the issue of scale-up further, one case of 4 in.−1 in. was scaled up from 1 in.−$^1/_4$ in. Three cases were considered with a constant velocity ratio. The velocity ratio was kept constant either by (i) keeping both velocities constant, which means that the values of the Reynolds number were increased by a factor of 4, (ii) keeping both flow rates constant, which means that the values of the Reynolds number were reduced by a factor of 4, or (iii) keeping the Reynolds number constant, which means that the flow rates were increased by a factor of 4 in order to keep U_j/U_m constant. Table 2 shows typical data for the above third case. The 95% mixing length for all three cases was found to be constant as shown in Table 3.

A case with a main velocity of 1 m/s and a side velocity of 17.1 m/s was also simulated for the 16 in.−1 in. case for U_j/U_m of 17.1. The 95% mixing length was found to be 9.5 diameters, which is the same for the base case of U_j/U_m of 17.1 where U_m is 0.23 m/s and U_j is 3.933 m/s. This shows that the 95% mixing length is affected by the velocity ratio and not by the individual values of the velocities.

Conclusions

Mixing of cold and warm water in pipelines with side and opposed tees was experimentally and numerically investigated. A good agreement between the experimental and numerical results is observed. The numerical and experimental values of the temperature distribution and the distance required to achieve 95% mixing are almost identical. The RSM and the $k-\epsilon$ model were used to account for turbulence and gave similar results except in the vicinity of the jet impingement region.

Results showed that the pipe length required to achieve 95% mixing is a strong function of the ratio of U_j/U_m and the angle of injection. A jet centered along the axis of the main pipe gives the shortest mixing length. The mixing length decreases as the velocity ratio increases. The rate of change becomes slower at velocity ratios higher than 30. For certain velocity ratios, the 95% mixing length may start to increase if the velocity ratio is increased over a threshold value. The angle of injection had a significant impact on the mixing length. A 90° jet angle showed the strongest impingememnt on the opposite walls. For a velocity ratio of 17.1, the 95% mixing length was found to be the shortest for an angle of 45 or 165°. This optimum angle is likely to change for a different velocity ratio. The mixing length is a function of U_j/U_m and d_j/d_m. The individual values of the velocities and pipe diameters did not have a significant impact on the mixing length. For constant d_j/d_m and U_j/U_m, the 95% mixing length is independent of the value of the Reynolds number.

Acknowledgment

The authors are grateful for the funding and support provided by King Fahd University of Petroleum & Minerals during the course of this work and the preparation of this paper.

Literature Cited

(1) Simpson, L. L. In *Turbulence in Mixing Operations*; Brodkey, R. S., Ed.; Academic Press: New York, 1975.

(2) Gray, J. B. In *Mixing: Theory and Practice*; Gray, J. B., Uhl, V. W., Eds.; Academic Press: New York, 1986; Chapter 13, Vol. III.

(3) Forney, L. J. In *Encyclopedia of Fluid Mechanics*; Cheremisinoff, N. P., Ed.; Gulf Publishing Co.: Houston, TX, Chapter 25, Vol. II.

(4) Liou, T.-M.; Liao, C.-C.; Chen, S.-H.; Lin, H.-M. Study on Side-Jet Injection near a Duct Entry with Various Injection Angles. *Trans. ASME* **1999**, *121*, 580.

(5) Weber, L. J.; Schumate, E. D.; Mawer, N. Experiments on Flow at a 90° Open-Channel Junction. *J. Hydraul. Eng.* **2001**, *127*, 340.

(6) Lam, K. M.; Xia, L. P. Experimental Simulation of a Vertical Round Jet Issuing into an Unsteady Cross-Flow. *J. Hydraul. Eng.* **2001**, *127*, 369.

(7) Pan, G.; Meng, H. Experimental Study of Turbulent Mixing in a Tee Mixer Using PIV and PLIF. *AIChE J.* **2001**, *47*, 2653.

(8) Moussa, Z.; Trischka, J.; Eskinazi, S. The Near Field in the Mixing of a round Jet with a Cross Stream. *J. Fluid Mech.* **1977**, *80*, 49.

(9) Crabb, D.; Durao, D.; Whitelaw, J. H. A Round Jet Normal to a Cross Flow. *J. Fluids Eng.* **1981**, *103*, 143.

(10) Cozewith, C.; Ver Strate, G.; Dalton, T. J.; Frederick, J. W.; Ponzi, P. R. Computer Simulation of Tee Mixers for Non-Reactive and Reactive Flows. *Ind. Eng. Chem. Res.* **1991**, *30*, 270.

(11) Forney, L. J.; Monclova, L. A. Numerical Simulation of Pipeline Tee Mixers: Comparison with Data. In *Industrial Mixing Technology: Chemical and Biological Applications*; Gaden, E. L., Tatterson, G. B., Calabrese, R. V., Penney, W. R., Eds.; p 141.

(12) Cozewith, C.; Busko, M. Design Co-Relations for Mixing Tees. *Ind. Eng. Chem. Res.* **1989**, *28*, 1521.

(13) Sroka, L. M.; Forney, L. J. Fluid Mixing with a Pipeline Tee: Theory and experiment. *AIChE J.* **1989**, *35*, 212.

(14) Sroka, L. M.; Forney, L. J. Fluid Mixing in a 90° Pipeline Elbow. *Ind. Eng. Chem. Res.* **1989**, *28*, 850.

(15) Maruyama, T.; Suzuki, S.; Mizushina, T. Pipeline Mixing between Two Fluid streams Meeting at a T-Junction. *Int. Chem. Eng.* **1981**, *21*, 205.

(16) Feng, Z.; Wang, X.; Forney, L. J. Single Jet Mixing at Arbitrary Angle in Turbulent Tube Flow. *Trans. ASME* **1999**, *121*, 762.

(17) Jayanti, S. Hydrodynamics of Jet Mixing in Vessels. *Chem. Eng. Sci.* **2001**, *56*, 193.

(18) Zughbi, H. D.; Rakib, M. A. Numerical Simulations of Mixing in a Fluid Jet Agitated Tank. *Chem. Eng. Commun.* **2002**, *189*, 1038.

(19) Patwardhan, A. W. CFD modeling of jet mixed tanks. *Chem. Eng. Sci.* **2002**, *57*, 1307.

Received for review December 6, 2002
Revised manuscript received July 7, 2003
Accepted July 10, 2003

IE0209935